Polyimide-Silica Hybrids: Spectroscopy, Morphology and Mechanical Properties

Mario Abbate,[1] *Pellegrino Musto,**[1] *Giuseppe Ragosta,*[1] *Gennaro Scarinzi,*[1] *Leno Mascia*[2]

[1]Institute of Chemistry and Technology of Polymers (ICTP), National Research Council of Italy, Via Campi Flegrei 34, Olivetti Building 70, 80078 Pozzuoli, NA, Italy
E-mail: musto@irtemp.na.cnr.it
[2]Institute of Polymer Technology and Materials Engineering, University of Loughborough, Loughborough, LE11 3TU, UK

Summary: Polyimide/silica hybrids were prepared by a sol-gel process and were evaluated in terms of curing behaviour, morphology and mechanical properties. The spectroscopic examination showed that the presence of the inorganic phase accelerates the imidization of the polyamic acid. Two types of morphology for the silica phase were obtained by tailoring the composition of the precursor solution mixture. The mechanical properties were found to be strongly dependent on the system morphology. The largest increase in rigidity and strength properties were achieved when the two phases were co-continuous.

Keywords: FTIR; mechanical properties; nanocomposites; polyimide

Introduction

Polyimides are well known for their excellent thermal stability and mechanical properties[1-3], and are widely used in electrical and electronic applications[4]. More recently, these polymers have been used as matrices for hybrid organic/inorganic (O-I) systems[5-8]. O-I hybrid systems are an important class of new-generation materials which combine the desirable properties of a ceramic phase (heat resistance, retention of mechanical properties at high temperatures and low thermal expansion) and those of organic polymers (toughness, ductility and processability). Among the various approaches used to produce hybrid composites, the sol-gel route provides a unique and versatile method. It can be viewed as a two-step network forming process, the first step being the hydrolysis of a metal alkoxide and the second consisting of a polycondensation reaction[9, 10]. Polyimides are particularly suitable for this type of process since they can be produced from

 DOI: 10.1002/masy.200451422

polyamic acid precursors which are soluble in hygroscopic solvents and can, therefore, tolerate the addition of water necessary to accomplish the hydrolysis of the alkoxide.

In the present study polyimide/silica hybrid materials were prepared by the sol-gel route, and characterized in terms of their curing behaviour, morphology and mechanical properties. Micron sized particulate composites were produced by using an additive-free TEOS solution, while nano-structured, co-continuous nanocomposites were obtained by introducing a suitable coupling agent (GOTMS) in the precursor solution for the silica phase.

Experimental

The polyimide precursor used in this study was Pyre-ML RK 692 from I.S.T (Indian Orchard, MA), commercially available as a 12 wt % solution in a mixture of N-methyl-2-pyrrolidone (NMP) and xylene (weight ratio 80/20). The precursor was a polyamic acid (PAA) formed by condensation of pyromellitic dianhydride (PMDA) and oxydianiline (ODA) having $\overline{M}_w = 1.0 \cdot 10^5$ and $\overline{M}_n = 4.6 \cdot 10^4$. High purity grades of tetraethoxysilane (TEOS) and γ-glycidyloxypropyltrime-thoxysilane (GOTMS) were obtained from Aldrich (Milwaukee, WI). Distilled water was used to induce hydrolysis of the alkoxysilane components using a 32 wt % HCl solution as catalyst and ethanol as solvent.

The alkoxysilane solutions used for the production of the polymer-silica hybrid films were prepared from either pure TEOS or TEOS/GOTMS mixtures. In a typical formulation (22.2 wt % of silica) 3.46 g of TEOS, 0.86 g of EtOH, 1.20 g of GOTMS, 082 g of H_2O and 0.12 g of an aqueous HCl solution (2.0 wt %) were added sequentially in a glass vial. The mixture was magnetically stirred at room temperature (RT), until a clear solution was obtained. The precursor hybrid solution was subsequently obtained by adding dropwise the hydrolysed alkoxysilane solution to the polyamic acid solution, under continuous stirring for 10 min at RT.

The procedure for the film preparation is reported in detail elsewhere[11].

Transmission FTIR spectra were obtained using a System 2000 spectrometer from Perkin-Elmer (Norwalk, CT). This instrument employs a Germanium/KBr beam splitter and a deuterated tryglycine sulfate (DTGS) detector. Small dumb-bell specimens with waist dimensions of 20 x 3.5 mm were used for tensile mechanical tests. The specimens were tested at ambient temperature using an Instron instrument (mod. 4505) at a cross-head speed of 1 mm min^{-1}. At least five

specimens were tested at each temperature. Stress-strain curves were recorded from which the modulus, the stress and the elongation at fracture were evaluated. The fractured surfaces of films obtained after cooling in liquid nitrogen were examined by scanning electron microscopy (SEM). The apparatus used was a Philip SEM mod. XL20 and the fracture surfaces were coated with a gold-palladium layer by vacuum sputtering.

Results and discussion

FTIR Spectroscopy

The kinetics of thermal imidization was evaluated spectroscopically by considering the evolution of the imide band at 1376 cm^{-1}. The spectra in the wavenumber range 1480 – 1280 cm^{-1}, collected at different times during the isothermal curing at 120°C for the polyimide precursor are shown in Fig. 1.

From the above spectra it is possible to evaluate the imidization degree, *i.d.*, as:

$$i.d.(t) = \frac{\overline{A}_t(1376)}{\overline{A}_f(1376)} \qquad 1)$$

where $\overline{A}_t(1376)$ is the normalized absorbance of the 1376 cm^{-1} band [i.e. $A_t(1376)/A_t(1498)$] at time t and $\overline{A}_f(1376)$ is the normalized absorbance of the same band after full cure of the polyimide. The i.d. parameter, relative to three different systems, is reported in Fig. 2 as a function of the reaction time. In particular, curve A refers to a nanocomposite with 22.2 wt % of silica, curve B is for the pure polyimide precursor and curve C is relative to a PAA film from which the NMP solvent was completely removed before curing, according to a procedure described in Ref. 12. The kinetic data for the imidization of the polyimide precursor, shown in Fig. 2, curve B, are in general agreement with other published results. In particular, two distinct regimes can be distinguished, both being adequately described as first order processes. The initial regime is faster than the second by a factor of about 6.5. The kinetic constants evaluated for PAA and for the nanocomposite are collectively reported in Table I. It is also worth to note that partial imidization (*i.d.* = 0.06) takes place during the heating ramp before reaching the isothermal temperature. For this reason the conversion curve does not start from the origin.

Several explanations have been put forward to account for the decrease of the cyclization rate at higher conversion and for the characteristic two-stage behaviour of the polyimide precursor.

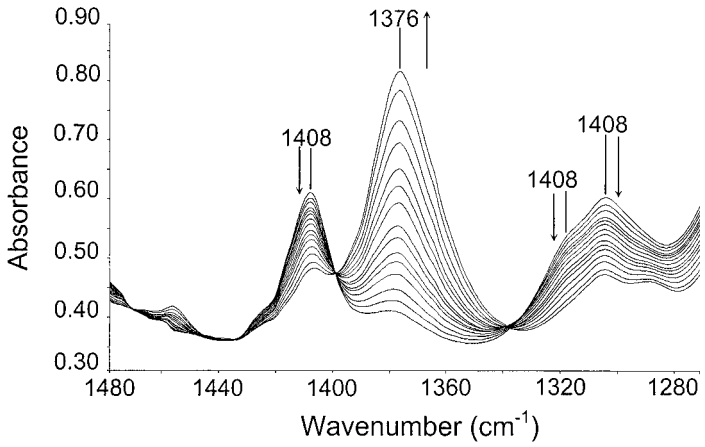

Fig. 1. Transmission FTIR spectra in the wavenumber range 1480 – 1280 cm^{-1} collected at various times during the isothermal imidization of the polyimide precursor at 120°C.

The principal arguments are:

In PAA the amic acid groups are in two non-equivalent kinetic states, differing in their conformation. One state is activated for cyclization while the other is not. The activated state rapidly cyclize during the first stage, while the remaining inactive groups react in the second stage[13, 14].

The imidization reaction is enhanced by the presence of solvent. Therefore, the decrease in reaction rate is due to the gradual loss of residual solvent from the system[15, 16].

As the cyclization proceeds, the T_g of the system increases, so that the polymer undergoes a rubber-to-glass transition. Since the transition from an unfavourable to a favourable conformation of the amic acid groups requires a rotation around a bond of the polymer chain, a decrease of the overall molecular mobility will reduce the rate of formation of active sites and hence the imidization rate[15-18].

The data shown in Fig. 2, curve C, relative to a PAA film from which all NMP had been eliminated prior to curing, confirm the fundamental role of residual solvent in the cure kinetics of

polyimides. In fact, a drastic reduction of the imidization rate is observed in comparison to the control system (compare curves B and C).

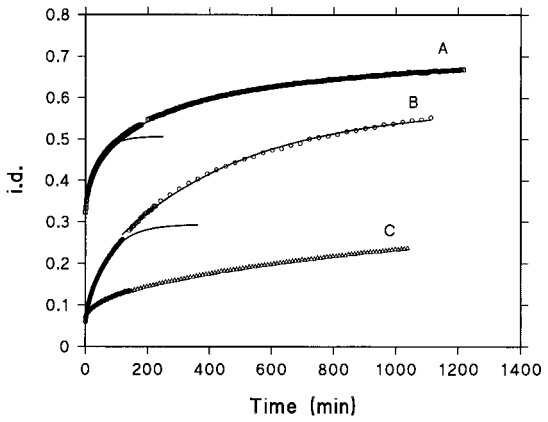

Fig. 2. Imidization degree (i.d.) as a function of time for the isothermal reaction at 120°C. Curve A: The PAA/TEOS/GOTM solution yielding the hybrid system with 22.0 wt % of silica (nanocomposite); Curve B: the polyimide precursor; Curve C: the polyimide precursor from which the solvent had been completely eliminated prior to curing. The symbols indicate the experimental data, while the continuous lines represent the simulations of the first order kinetic model.

Table I. Parameters obtained from the kinetic analysis of the imidization reaction.

Code		k_i (min^{-1})	$\frac{C_i - C_0}{C_i}$	$\frac{C_i - C_f}{C_i}$	R^2
PAA	First regime	0.015	0.06	0.24	0.997
	Second regime	0.0023	-	0.58	0.999
Nanocomposite	First regime	0.023	0.33	0.51	0.997
(22.0 wt % silica)	Second regime	0.0028	-	0.67	0.999

A fast initial imidization stage can still be distinguished and again the reaction starts below 120°C, suggesting that a certain amount of amic acid groups are present as active species. However, their concentration is very low in comparison to the solvent containing system, as demonstrated by the shorter duration of the initial stage and the lower conversion attained at the end of this regime. As the active groups are fully consumed, the reaction rate drops dramatically;

in fact, in the absence of solvent which acts a an efficient plasticizer, the T_g of the material is high and the required conformational transition is strongly hindered.

The kinetic behaviour of the nanocomposite precursor resembles that of the pure polyamic acid in presence of solvent, in that it can be adequately described by two first-order regimes. The second of which has a rate constant considerably lower than the first. However, in the nanocomposite system the first stage is significantly faster than for the pure polyamic acid in solution (see the kinetic parameters collected in Table I) and the imidization reaches a more advanced stage during the heating ramp from room temperature to 120°C. The initial conversion of amic acid groups is 0.33 for the nanocomposite system and only 0.06 for the polyamic acid solution. As a consequence of these two effects the final conversion of amic acid is higher in the nanocomposite than in the pure polyimide polyimide (0.67 against 0.58). The second stage of imidization in the two systems, however, is characterized by a comparable rate constant.

The kinetic behaviour for the nanocomposite precursor seems to be conflicting with the solvent effect, since it has been demonstrated in previous investigations[6] that the residual amount of solvent is much lower in the nanocomposite formulation than in the in pure polyamic acid solution. Evidently, the inorganic phase exerts a catalytic activity with respect to the imidization of polyamic acid; a possible explanation for this effect can be related to the large amount of hydroxyl groups present along the outer surface of the silica phase. These groups may form strong molecular interactions of the hydrogen bonding type with the amic acid moieties of PAA. In doing so, the PAA chains may be forced to assume a planar conformation more favourable for cyclization.

Mechanical properties and morphology

Stress-strain parameters evaluated at ambient temperature for the polyimide and for the polyimide/silica hybrids are reported in Figs 3-5. The modulus is found to increase linearly with increasing the concentration of the inorganic phase (Fig. 3). In particular a maximum enhancement by a factor of about two is obtained for a silica concentration of 28.4 %. The plot of the tensile strength as a function of the silica concentration (Fig. 4) displays a gradual increase up to a silica content around 20 wt %, followed by a slight reduction at higher concentrations. The elongation at break, reported in the same figure, exhibits a monotonic decrease. In Fig. 5 are shown the mechanical properties expressed in terms of tensile strength and elongation at break,

for hybrid systems obtained without the compatibilising agent (GOTMS). One notes that the tensile strength does not show the initial increase observed for the compatibilised systems, but decreases gradually over the whole composition range. The elongation at break displays a behavior very close to that of the nanocomposite formulations.

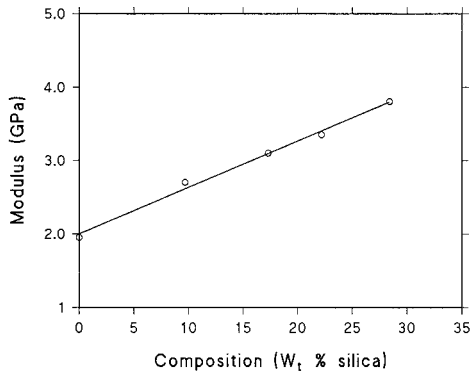

Fig. 3. Elastic modulus for the hybrid systems prepared from PAA/TEOS/GOTM solutions (nanocomposites), as a function of the silica content.

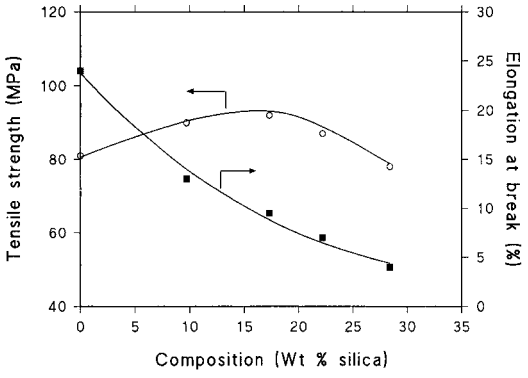

Fig. 4. Strength and elongation at break for the hybrid systems prepared from PAA/TEOS/GOTM solutions (nanocomposites), as a function of the silica content.

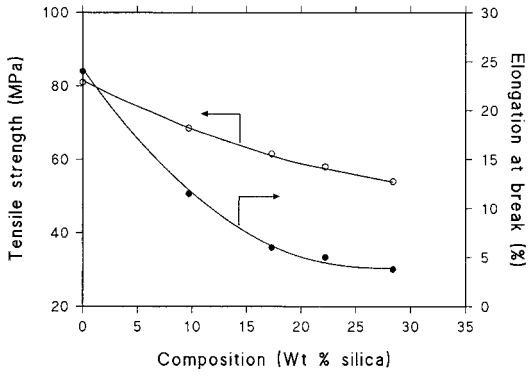

Fig. 5. Strength and elongation at break for the hybrid systems prepared from PAA/TEOS solutions (microcomposites), as a function of the silica content.

It is known that in polymeric composites the external stress is transferred from the continuous polymeric matrix to the discontinuous reinforcing phase[19, 20]. Thus, the ultimate properties of composite materials are dependent on the extent of bonding between the two phases, as well as on the surface area and the geometry of the reinforcing phase.

In Fig. 6 are shown the scanning electron micrographs of polyimide-silica mixtures obtained with and without the addition of GOTMS. These micrographs show clearly the effect of GOTMS, which brings about a morphological transition from a dispersed-particle phase structure (Fig. 6A), in the absence of GOTMS, to a fine interconnected or co-continuous phase morphology (Fig. 6B), with the use of GOTMS. For the compatibilised system the size of the interconnected silica domains ranges from 40 to 100 nm, while for the non-compatibilized system, the average diameter of the silica particles varies from 1 to 2 μm.

The micrograph of Fig. 6A also reveals that the silica particles are very smooth and completely debonded from the surrounding polyimide matrix, indicating a poor interfacial adhesion between the two phases.

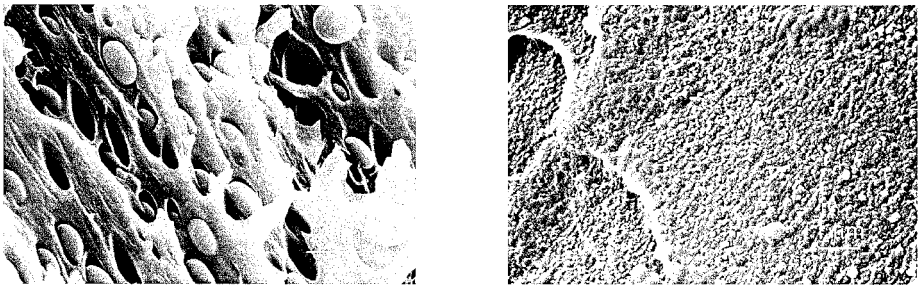

Fig. 6. SEM micrographs for the microcomposite (A) and for the nanocomposite (B) containing 22.2 wt % of silica.

On the basis of these morphological observations, it is evident that the reduction in ultimate properties observed for non-compatibilized systems can be attributed to weak interactions between the phases, which allow the silica particles to act as stress-concentration defects, rather than as effective reinforcing fillers. On the contrary, for compatibilized systems, the increased tensile strength is the result of both a better interfacial adhesion and the formation of co-continuous morphologies, which improve the efficiency of stress transfer mechanisms between the two components. In spite of the enhanced adhesion, the elongation at break decreases since the interconnected silica phase hinder the plastic flow of the polyimide phase, preventing large deformations to occur prior to fracture.

Conclusions

A number of polyimide/silica hybrid systems have been prepared and characterized with respect to their curing behaviour, morphology and mechanical performances. A sol-gel type of process has been employed to produce nanocomposite structures or more conventional two-phase composites. A time-resolved spectroscopic analysis has pointed out that the presence of the silica precursor within the pre-polymer solution considerably accelerates the imidization of the polyamic acid. In terms of mechanical properties, it is found that a co-continuous phase morphology with high adhesion between the phases brings about a general improvement of most mechanical parameters with respect to both the plain polyimide and hybrid systems where the inorganic phase forms discrete, micron sized domains with no adhesion to the polymer matrix.

1. Gosh M.K., Mittal K.L., *Polyimides; Fundamentals and Applications*, Marcel Dekker, New York, **1996**.

2. Feger C., Polyimides: Trends in Materials and Applications, Society of Plastic Engineers, New York, **1996**.

3. Bessonov M.I., Zubkov V.A., Polyamic Acids and Polyimides: Synthesis, Transformation and Structure, CRC Press, Boca Raton, **1993**.

4.Thompson L.F., Willson C.G., Tagawa S., *Polymers for Microelectronics: Resists and Dielectrics*, ACS Symposium Series 537, ACS, Washington DC, **1994**.

5. Mascia L., *Trends Polym. Sci.*, **1995**, *3*, 61.

6. Morikawa A., Iyoku Y., Kakimoto M., Imal Y., *Polym. J.*, **1992**, *24*, 107.

7. Nandi M., Conklin J.A., Salvati Jr. L. Sen A., *Chem. Mater.*, **1991**, *3*, 201.

8. Kioul A., Mascia L., *J. Non-Cryst. Solids*, **1994**, *175*, 169.

9. Strawbridge I.in *Chemistry of Glasses*, Paul A. Ed. Chapman and Hall, **1990**.

10. Huang H., Glaser R.H., Wilkes G.L. in *Inorganic and Organometallic Polymers*, Zeldin M., Winne K.J., Allcock H.R. Eds., ACS Symp. Series 360, ACS Washington DC, **1987**.

11. P. Musto, G. Ragosta, G. Scarinzi, L. Mascia, *Polymer*, in print.

12. Numata S., Fujisaki K., Kinjo N. in *Polyimides, Synthesis, Characterization and Applications*, Mittal K. Ed., Plenum, New York, **1984**, p. 259.

13. Laius L.A., Tsapovetsky M.I. in *Polyimides, Synthesis, Characterization and Applications*, Mittal K. Ed., Plenum, New York, **1984**, p. 311.

14. Laius L.A., Bessonov M.I., Kallistova E.V., Androva N.A., Florinsky F.S., *Vysokomol. Soedin.*, **1967**, *9A*, 2185.

15. Frayer P.D. in *Polyimides, Synthesis, Characterization and Applications*, Mittal K. Ed., Plenum, New York, **1984**, p. 273.

16. Gillham J.K., Gillham H.C., *Polym. Eng. Sci.*, **1973**, *13*, 447.

17. Laius L.A., Bessonov M.I., Florinsky F.S., *Polym. Sci. USSR*, **1971**, *13*, 2257.

18. Koton M.M., *Polym. Sci. USSR*, **1971**, *13*, 1513.

19. Clegg D.W., Collier A.A., Mechanical Properties of Reinforced Thermoplastics, Elsevier, London, **1986**.

20. Hornsby P.R., Hinrichsen E., Tarverdi K., *J. Mater. Sci.*, **1997**, *32*, 443.